Polymer 50 (2009) 5589–5597

Contents lists available at ScienceDirect

Polymer

journal homepage: www.elsevier.com/locate/polymer

Structural evolution of aging agar-gelatin co-hydrogels

S. Santinath Singh [a], V.K. Aswal [b], H.B. Bohidar [a,*]

[a] Polymer and Biophysics Lab, School of Physical Sciences, Jawaharlal Nehru University, New Delhi-110 067, India
[b] Solid State Physics Division, Bhaba Atomic Research Centre, Mumbai-400 085, India

ARTICLE INFO

Article history:
Received 7 April 2009
Accepted 12 September 2009
Available online 22 September 2009

Keywords:
Agar-gelatin
Co-hydrogel
Non-ergodicity

ABSTRACT

Agar-gelatin co-hydrogel was investigated over a period of ≈30-days by dynamic light and small angle neutron scattering, and rheology to quantify changes occurring inside the hydrogel. Degree of non-ergodicity was extracted as a heterodyne contribution from the measured dynamic structure factor data. From the analysis of the data, we observed two relaxation modes namely fast and slow modes with relaxation times τ_f and τ_s whose dependence with aging time, t_a fall on a scaling behavior given by power-laws, $\tau_f \sim (t_a)^{-1/5}$ and $\tau_s \sim (t_a)^{3/5}$ respectively. Further the analysis showed the heterogeneity size (ξ_{SANS}) obtained from SANS also follows power-law behavior, $\xi_{SANS} \sim (t_a)^{-1/5}$. The data taken together revealed the "speeding up" of fast and "slowing down" of slow mode relaxation processes.

1. Introduction

Novel and smart soft materials like polymer and colloidal gels, glasses, inter penetrating network structures (IPNS) and poly-electrolyte complexes (coacervates) have generated adequate interest in the recent past due to their enormous application potential [1–10]. Polymer gels constitute a special class of soft matter as far as their supramolecular structure and viscoelastic properties are concerned. A gel can be defined as a three dimensional interconnected percolating (mechanically) network structure with the continuous phase (solvent) interacting synergistically with the network [11]. The dispersed phase (polymer) can be present in a disordered and non-ergodic state. Regardless, these disordered systems are often found to be trapped far away from equilibrium, and typically relax slowly, exhibiting complex and interesting dynamics. Moreover, aging effects make the dynamics slow down significantly and often the response functions could still be scaled onto a master curve [3].

Physical gels and complex networks made of two (bio)-polymers (often called co-gels) produce new biomaterials with customized and controlled properties. Sodium caseinate-β-glucan gels generate a bi-continuous topology governed by the mechanical strength and thermal stability of the β-glucan network structure [12]. Agar-κ-carrageenan co-gels were characterized by rheology and it was found that incorporation of κ-carrageenan reduced gel rigidity (Young's modulus) significantly. Moreover, distinctive agar and κ-carrageenan polymer-rich zones, well segregated inside the gel phase, were observed with the agar-rich phase providing the continuous phase and κ-carrageenan-rich phase constituting the discontinuous gel phase [13]. Pectin-chitosan co-gels were studied and their phase stability behaviour was investigated. It was concluded that though the gel strength was dependent on the mixing ratio of the two polymers, the relaxation behaviour and microscopic geometrical structure (fractal dimension of the network) remained invariant of the same [4]. In earlier studies involving co-gels of agar-gelatin (biopolymers had concentrations far above their gelation concentration), it was concluded that phase separated micro-domains of the two biopolymers was formed inside the co-gel phase [14,15]. All these studies imply that it is possible to generate new soft biomaterials by adjusting the mixing ratio of two intelligently chosen biopolymers.

The co-gels, thus generated, often exhibit profound aging effect. In fact during sol-gel transition the incipient gel network is trapped in an inhomogeneous and non-ergodic state which slowly relaxes to an equilibrium state over an extended period of time which is characteristic of the synergistic interactions taking place inside the gel phase [1,2]. Aging effect has been observed in a variety of synthetic polymer, biopolymer and colloidal gels. Polycarbonate of bisphenol-A was studied for a period of 30 months at room temperature which indicated that the elastic modulus and hardness increased in a step-wise manner while the molecular weight distribution became broader with aging [16]. A variety of silica and doped silica gels have shown significant change in their thermal and rheological characteristics with aging [17–19]. Confocal scanning laser microscopy and permeametry experiments performed on aging rennet (-induced) casein gels reveal considerable coarsening of the gel structure and pore size increase with aging [20]. Human

* Corresponding author. Tel.: +91 11 26704637; fax: +91 11 2671 7537.
E-mail address: bohi0700@mail.jnu.ac.in (H.B. Bohidar).

0032-3861/$ – see front matter © 2009 Elsevier Ltd. All rights reserved.
doi:10.1016/j.polymer.2009.09.032

serum albumin trapped inside a tetraethyl orthosilicate bio-glass showed age dependent protein denaturation and partial inaccessibility of the protein to negatively charged species [21]. Mechanical properties of bacterial copolyester poly (3-hydroxybutyrate-co-3-hydroxyhexanoate) changed significantly with aging and gave rise to secondary crystallization [22]. Aging induced changes in the physical and mechanical properties observed in colloidal gels revealed quite interesting universal features [1–3].

Thus, study of aging in co-gels of biopolymers can be argued to have sufficient significance. In this work we have continuously and systematically monitored the temporal evolution of co-gels of a polypeptide (gelatin having concentration below its gelation concentration) and a polysaccharide (agar having concentration higher than its gelling concentration) over a period of ≈30 days using an array of experimental techniques like: DLS, SANS and rheology. The objective was to map how the incipient agar gel would phase separate. Gelatin is a polyampholyte prepared by hydrolytic degradation of collagen [23]. In the sol state, gelatin has a random coil conformation; the molecule is rich in glycine, proline and hydroxyproline sequences. In the gel state, three such molecules are joined by intermolecular hydrogen bonding provided mainly by the glycine which occurs at every third residue to form inter twined triple-helix structures. Individual gelatin molecules occur in the poly(L-proline II-trans) helical conformation [23] inside the triple-helix. Agar comprises mainly of alternating β-(1-4)-D and α-(1-4)-L linked galactose residues in a way that most of α-(1-4) residues are modified by the presence of a 3,6 anhydro bridge [23]. Other modifications commonly observed are mainly substitutes of sulphate, pyruvate, urinate or methoxyl groups. The gelation temperature of agar is primarily decided by the methoxy content of the sample. Agar sols form thermoreversible physical gels with large hysteresis between melting and gelling temperatures with the constituent unit being anti-symmetric double helices [25,26].

2. Materials and methods

We used gelatin sample of Type-A (porcine skin extract, bloom strength 300 and nominal molecular weight 100 kDa. Isoelectric pH = 9) obtained from Sigma Chemicals (USA). The gelatin sample was used as supplied. All other chemicals used were of analytical grade, brought from Thomas Baker, India. The solvent used was deionized water and ionic strength of the solvent was first set as per the experimental requirement (0.05 M NaCl). The gelatin solution (1.5% w/v, gelation concentration ≈2%) was prepared by dispersing gelatin in this medium at 60 °C. The macromolecules were allowed to hydrate completely; this took 30 min to 1 h. Gelatin solution undergo gelation transition [23] at a temperature ≈30 °C. Agar used in this study was extracted from the red seaweed *Gracilaria edulis* collected from the Gulf of Mannar at the southeast coast of India, employing the method described by Craigie and Leigh [24]. The agar had the following properties: gel strength 100 g/cm^2 (0.1% w/v gel at 20 °C); gelling temperature ≈36 °C and melting temperature ≈85 °C. The estimated molecular weight was ≈120–150 kDa. Agar solution (1.5% w/v, gelation concentration ≈0.1% w/v) was prepared in an autoclave using the same solvent. Both agar and gelatin solutions looked optically transparent at this temperatures. The mixing ratio [agar]:[gelatin] = 1, and NaCl salt concentration for both the solutions was 0.05 M. The mixed sol (pH = 5.4) was stirred at 60 °C for 30 min and, then was allowed to cool to room temperature (25 °C) that formed the required co-gel within an hour. The measurements started 3 days after sample preparation and were continued for next ≈30 days. The data pertaining to the measured parameters on the first and the last days are referred to in the text as initial and final values. The choice of gel concentration and mixing ratio was arbitrary.

DLS measurements were performed on the co-sol at 50 °C for the determination of the heterodyne parameter and the same for co-gel samples were performed at room temperature (25 °C). The sample was loaded into 5 ml clean optical quality borosilicate cylindrical glass cell and this cell was held inside a double walled temperature bath and temperature regulation was achieved by connecting this to a Grant, UK refrigerated circulating temperature controller that had an accuracy of ±0.1 °C. The scattered light from the sample was detected by the photomultiplier tube, and the photocurrent was suitably amplified and digitized before it was fed to a 1024 channel digital correlator (Brookhaven Instruments Inc., USA,model BI-9000AT). The whole scattering apparatus was placed on a vibration isolation table (Newport Corp.,USA). In all the experiments, the difference between the measured and calculated base line was not allowed to go beyond ±0.1%. The data that showed excessive baseline difference were rejected. The probe length scale is defined by the inverse of the modulus of the scattering wave vector q where the wave vector $q = (4\pi n/\lambda)\sin(\theta/2)$, the medium refractive index is n. The DLS experiments were mostly carried out at a fixed angle 90°.

For SANS study samples were prepared in D_2O to minimize incoherent background. SANS is a diffraction technique which involves scattering of a monochromatic beam of neutrons from the sample and measuring the scattered neutron intensity as a function of the scattering angle. These experiments were performed on the spectrometer at the G.T. laboratory, Dhruva reactor (Bhaba Atomic Centre, Trombay, India). Further details of the SANS spectrometer at Dhruva are discussed elsewhere [27]. The wave length of the neutrons used covered the scattering vector (q) range

$$7 \times 10^{-3}\text{Å}^{-1} \leq q \leq 3 \times 10^{-1}\text{Å}^{-1}$$

Where $q = (4\pi/\lambda)\sin(\theta/2)$, λ is the wave length of neutron and θ is the scattering angle. The mixed solution before forming co-gel was transferred to quartz cell thickness 2 mm and scattered intensity was measured as function of scattering vector. The measured intensity was corrected for the background and the empty cell contribution, and the data were normalized to get the structure factors. The raw data were corrected for background, sample cell and electronic noise by conventional procedure. Furthermore, the two-dimensional isotropic scattering data were azimuthally averaged. This was converted to an arbitrary unit scale using the incoherent scattering data of pure water. The details of the data normalization procedure are discussed elsewhere [27].

Rheology measurements were performed using an AR-500 model stress controlled rheometer (T.A. Instruments, UK). The sample was kept on the Peltier plate with a temperature stability ±0.1 °C and a homemade sponge solvent trap was used to reduce evaporation of the solvent. The measuring geometry was a 20 mm, 2° cone-plate arrangement having a truncation gap of 51 μm. The sample was subjected to sinusoidal oscillations of frequency 1 Hz and the amplitude of the oscillation was controlled to obtain a 0.1% strain to the sample that the structure of agar-gelatin co-gel was not destroyed by the measurements. In the flow mode, the shear rate was from 0.01 to 100 s^{-1} and 1 °C/min was the heating rate for the temperature ramp measurements. The slip in the geometry was taken care of by adjusting the trim gap as per the procedure mentioned by the manufacturer.

3. Results and discussions

3.1 Non-ergodic behaviour

Polymer gels, intrinsically, are non-ergodic, which increases the complexity of data analysis associated with dynamic light

scattering experiments [26,28–30]. The standard analysis of light scattering data requires that the system is completely ergodic (means that time and ensemble averages are identical), and stationary (process is independent of origin of time) which is adequately satisfied only in case of scattering from dilute solutions. In order to make the DLS measurements compatible with the said requirements this problem was addressed in the following way. The normalized intensity correlation function, $g_2(q, t)$, obtained from the gel sample can be related to the dynamic structure factor, $g_1(q, t)$ as [28,29]

$$g_2(q,t) = 1 + \beta'\left[2X(1-X)g_1(q,t) + X^2\left|g_1(q,t)^2\right|\right] \quad (1)$$

where β' is the coherence factor having a maximum value of 1 and relates with the number of statistically independent speckles detected and/or amount of dynamic scattering within the time window. The parameter X ($0 \le X \le 1$) defines the ergodicity via the amount of heterodyne contribution present in the correlation data. Thus X accounts for the non-ergodic contribution buried in the measured data in a measurable way. Both β' and X are measurable parameters in a real experiment. The measured intensity auto-correlation data was analyzed exactly following the description given elsewhere [29]. For the gels, we found $X \approx 0.15 \pm 0.03$, independent of gel aging (see Fig. 1). Thus the pre-factor of the linear term in $g_1(q, t)$ in Eq. (1) is ≈20 times larger than the quadratic second term. This gave

$$g_1(q,t) = [g_2(q,t) - 1]/[2\beta' X(1-X)] \quad (2)$$

Any error thus accrued is absorbed as experimental error in subsequent data analysis. Fig. 1 clearly shows that the co-gel is trapped in a non-ergodic phase even after a lapse of 30 days. Similar observation of non-ergodicity and its temporal evolution has been reported with adequate quantitative analysis in incipient gelatin gels [30,31] and charged colloidal suspension gels [1] in the past. In fact, often the gel state is defined as one that is disordered and non-ergodic. The procedure adopted does not take into account contributions arising from very slow modes (frozen dynamics). A more rigorous approach involves tedious ensemble average over hundreds of speckles [30].

3.2 Analysis of dynamic structure factor (DLS data)

The exact evaluation of the dynamic structure factor, $g_1(q,t)$ from the measured intensity auto-correlation function was achieved after the non-ergodic contribution was removed from the experimental data as described in Eqs. (1) and (2); this is plotted in Fig. 2. This data, in principle can be fitted to a range of functional forms [32].

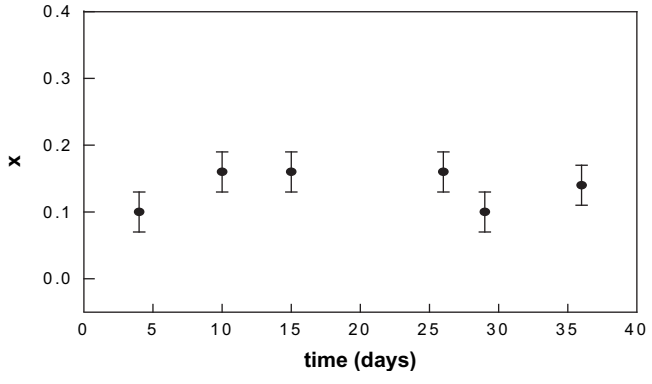

Fig. 1. Variation of non-ergodicity parameter X for agar-gelatin co-gel as function of gel age. The data clearly reveals the age invariance of non-ergodicity.

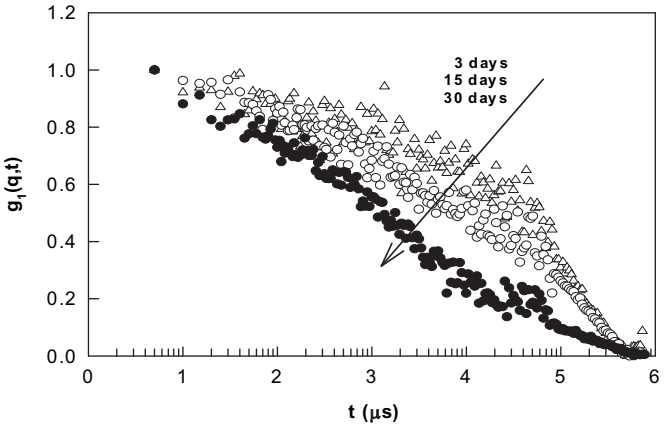

Fig. 2. Semi-log plot of dynamic structure factor evolving with gel aging. This data could be decomposed into fast and slow mode relaxations following the description given by Eq. (4). Notice that the data scatter reduces significantly as the gel ages. See text for more details.

In order to avoid over dependence on the Laplace inversion method, independently, unsuccessful attempt was made to fit the structure factor data to a single exponential and also to a three exponential relaxation mode (observed in some gels [33]) model with the intermediate mode being a power-law mode. This gave credence to the applicability of a two-mode relaxation process to the $g_1(q,t)$ data. Having confirmed this all $g_1(q,t)$ were least-squares fitted to the functional form

$$g_1(q,t) = A\exp\left(-t/\tau_f\right) + B\exp\left[-(t/\tau_s)^\beta\right] \quad (3)$$

Where, the fast (diffusivity $= D_f = 1/\tau_f q^2$) and slow modes (relaxation time $= \tau_s$) follow exponential and stretched exponential relaxation respectively. Here, A and B are amplitudes of the two relaxation modes, and β is the width of the slow mode relaxation function. It was not possible to fit the data to Eq. (3) because of unacceptably low χ^2 values. This forced us to use Eq. (4) where the χ^2 values consistently remained higher than 95%. The correlation data was analyzed through user defined least-squares fitting routines of SigmaPlot software (SPSS, USA). The $g_1(q,t)$ data was split as follows:

$$g_1(q,t) = \begin{cases} \exp(-D_f q^2 t); & t \le 500\mu s \quad \text{fast mode} \\ \exp\left(-(t/\tau_s)^\beta\right); & 500\mu s < t \le 1s \quad \text{slow mode} \end{cases} \quad (4)$$

The fast mode was found to be diffusive (data not shown) and the diffusivity is normally related to the characteristic length, ξ_{DLS} through Stoke–Einstein relation as [34]

$$D_f = k_B T/(6\pi\eta_0\xi_{DLS}) \quad (5)$$

Where solvent viscosity is η_0, k_B is Boltzmann's constant and T is absolute temperature. The fast mode component of the $g_1(q,t)$ data was fitted to Eq. (4) that yielded the value of D_f and allowed the determination of ξ_{DLS} values. The variation of characteristic length with aging time of the co-gel is shown in Fig. 3 which revealed ≈55% decrease in its value (from 22 nm to 12 nm) indicating "speeding up" of the fast mode dynamics. This can be identified as the mesh size of the agar double helix networks. Initially, such networks had a very rarified structure, but with the occurrence of aggregation and the concomitant syneresis, these shrink to more compact structures evolve asymptotically in time. The physical

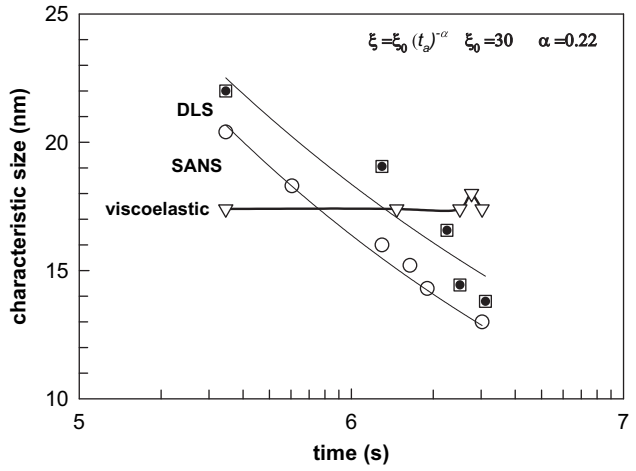

Fig. 3. Semi-log plot of characteristic size as function of gel age. The parameters ξ_{DLS} and ξ_{SANS} determined from light and neutron scattering data showed a universal power-law dependence on time, t_a given by the Eq. (13) (solid line). The viscoelastic length, however, remained invariant of gel aging indicating that this length scale did not capture the internal dynamics effectively. See text for details.

implication of variation of characteristic length with gel age will be discussed later. This behaviour must not be confused with the increase in correlation length observed in nascent agar gels until pseudo-equilibrium is reached [26].

The dynamic structure factor data for $t > 500\ \mu s$ was fitted to stretched exponential function defined in Eq. (4). This yielded the values for slow mode relaxation time (τ_s) and the width parameter (β). The dependence of these characteristic parameters on gel aging has been clearly shown in Fig. 4 which indicates that the values observed changed by $\approx 70\%$ as the co-gel aged to ≈ 30 days, but the relaxation time increased while width decreased. The τ_s values can be attributed to the relaxation of agar-gelatin complex network structures (as conjecture) which increased by $\approx 300\%$ as the co-gel aged to 30 days (Fig. 4). Agar is polyanionic [34] whereas gelatin is a polyampholyte carrying a net positive charge at $pH = 5.4 < pI = 9$. This enables screened coulomb interactions between agar and the oppositely charged gelatin molecules giving rise to intermolecular binding. Many such junctions can be located in a gelatin-rich domain which will readily bind with unreacted segments of agar molecules creating complex networks. The number density of such domains can be appreciably large and these are dispersed heterogeneously inside the co-gel matrix. The coalescence of these domains is not possible because these are locally bound to the continuous phase which is the pervading agar gel. It was not possible to determine a size parameter from slow mode data which could correspond to the size of complex network domains because the appropriate viscosity was unknown. It has been reported [34] that use of inaccurate solvent viscosity value can sufficiently distort the size parameters estimated from DLS experiments. The increase in complex network domain size can be explained as follows. The increase in slow mode relaxation time owes it origin to the osmotic swelling of the complex networks structures, again made possible due to the presence of solvent released by syneresis from the agar gel domains that are present in close vicinity. Such a process increases the entropy of the system and helps it to move towards equilibrium. The decrease in the β value implies the "slowing down" of slow mode relaxation process. The relative amplitudes of the fast and slow modes are shown in Fig. 5 which implies that both modes have same amplitude initially, but the fast mode slowly grows at the expense of the slow mode.

Thus, the data shown in Figs. 3 and 4 imply "speeding up" of the fast mode and "slowing down" of the slow mode. Since, the fast mode amplitude dominated the scattering (Fig. 5), the net result will be narrowing of the correlation function which can be visualized from the $g_1(q,t)$ data shown in Fig. 2.

3.3 Analysis of static structure factor (SANS)

The present objective was to study the microscopic structure of the agar-gelatin co-gels. The expression for scattering cross-section can be simplified for the experimental situation under consideration that permits the SANS data to be in two distinct ranges of scattering vectors (q): low-q range (Debye–Bueche behaviour [35]) and the intermediate-q range (Ornstein–Zernike behaviour [35]). Analysis of SANS data within the model of mean field theory reveals that for the polymers in a good solvent, at equilibrium, the structure factor of concentration fluctuations in the Ornstein–Zernike (O–Z) region is given by

$$S_L(q) = I_L(0)/(1 + q^2\xi_C^2); \quad q\xi_C \ll 1 \tag{6}$$

Where, ξ_C defines the correlation length of the concentration fluctuations or mesh size of the network and $I_L(0)$ is related to the

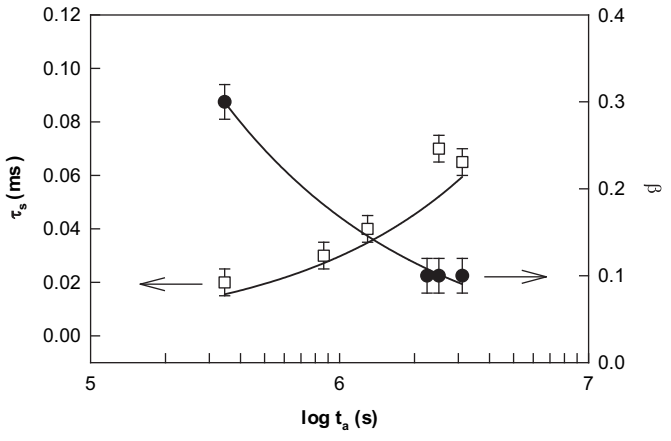

Fig. 4. Time dependence of slow mode relaxation time, τ_s and width parameter, β for agar-gelatin co-gel at room temperature. The temporal dependence could be adequately described by a power-law fitting to the function given by Eq. (14) (solid line). See text for details.

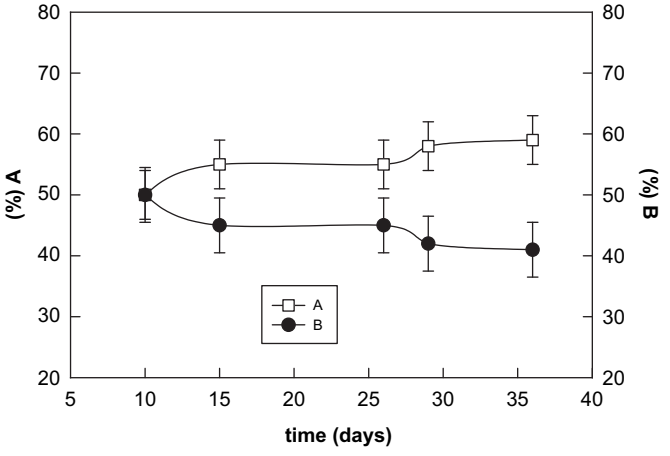

Fig. 5. Variation of fast (A) and slow (B) mode amplitudes of the dynamic structure factor data with gel age. Notice that, initially both processes had identical amplitudes, but with time evolution the fast mode starts to grow at the cost of the slow mode. Solid lines are guide to the eye.

crosslink density and longitudinal osmotic modulus. Experiments carried out in the semi dilute regime of polymer solutions have shown deviations from the Ornstein–Zernike function. It must be clarified here that Ornstein–Zernike formalism works for good solvents and for systems that are in equilibrium. Though, the co-gel state in itself is in non-equilibrium and is evolving with time to reach subsequent lower free-energy states, when it is in contact with its supernatant (which is always the case in experiments), it is in a state of dynamic equilibrium globally. Secondly, the dense phase is still considerably hydrated. Thus, application of Ornstein–Zernike model poses no serious problem.

Long wavelength concentration fluctuations in these systems often gives rise to "excess scattering" in the low-q region of the SANS data. If the spatial scale of density fluctuations due to the presence of such inhomogeneities of size ξ_{SANS} is large compared to the correlation length ξ_C, then the two contributions can be treated separately and added to give the total structure factor as

$$S(q) = S_L(q) + S_{ex}(q) \quad (7)$$

Where $S_L(q)$ is the Ornstein–Zernike (O–Z) function, and the Debye–Bueche (D–B) structure factor has the form $S_{ex}(q)$ given by

$$S_{ex}(q) = I_{ex}(0)/(1 + q^2\xi_{SANS}^2)^2 \quad (8)$$

where $I_{ex}(0)$ is the extrapolated structure factor at zero wave vector. It is possible to study low-q domain of the structure factor provided a high instrumental resolution SANS spectrometers is used to collect data.

A plot of $1/S(q)$ versus q^2 clearly distinguishes the domains where D–B and O–Z functions are operative (see Fig. 6). A least-squares fit of the structure factor data in the low-q range, $0.018\ \text{Å}^{-1} \le q \le 0.072\ \text{Å}^{-1}$, to the D–B function and the same in the intermediate-q range to O–Z function revealed a clear q-cutoff $= 0.072\ \text{Å}^{-1}$ (this showed no aging effect) and values for characteristic lengths, ξ_{SANS} and ξ_C. The correlation length value obtained was $\xi_C = 2.0$ nm initially that fell by 50% with time to reach a value 1.0 nm. These are too small values, but similar observations were made in agar-gelatin coacervate samples too [6]. On the other hand the size of inhomogeneities was $\xi_{SANS} = 21$ nm initially, which decreased to a final value ≈ 12 nm. Let us compare these values with some relevant data pertaining to agar and gelatin gels. The persistence length of gelatin is ≈ 2.5 nm. For gelatin gels and sols the correlation length values are reported [8] to be same and equals 2.6 nm. Size of heterogeneities reported for such systems were ≈ 20 nm which is comparable to the size of the heterogeneities observed, $\xi_{SANS} = 21 \pm 3$ nm. On the other hand, agar gels are associated with contrastingly different length scales; the correlation length and heterogeneity size are 5.9 nm and 70 nm respectively [6]. Thus, a cursory look indicates that the length scales observed in the co-gel system compares rather well with that of gelatin gel, at least in the early stage of aging. The temporal variation of ξ_{SANS} is plotted in Fig. 3 along with the ξ_{DLS} data obtained from light scattering experiments for comparison.

3.4 Viscoelastic behavior

The change in the viscoelastic behaviour of the co-gel with aging was probed by monitoring the following three parameters: gelation and melting temperature (isochronal temperature sweep studies), gel rigidity (isothermal frequency sweep studies) and gel fluidity (isothermal shear studies). In the temperature sweep experiments, storage (G′) and loss (G″) modulii were measured under isochronal conditions ($\omega = 3.5$ rad/s) and using a programmed ramp of 1 °C/min. The first derivative of the storage modulus with temperature (dG′/dT) yielded a peak corresponding to the characteristic temperatures where transitions were located. The derivatives are shown in the inset of Fig. 7 that shows variation of gelation (T_{gel}) and melting (T_m) temperatures with time. Both the temperatures could be seen to decrease with time. The melting temperature reduced by almost 50% as the co-gel was aged to 30 days. Agar-κ-carrageenan co-gels have shown identical behaviour [13]. The corresponding low frequency modulii values are plotted in Fig. 8 which, again, reveals reduction by $\approx 10\%$ and 20% for G′ and G″ respectively, in their values with gel aging. Thus, the two observations: reduction in T_m (and T_{gel}) and modulii values imply increased softening of the co-gel with aging. Usually gels and glasses become progressively stiffer with waiting time. Thus, the softening can be attributed to the formation of imperfect structures.

The shear rate dependent viscosity data of these samples is plotted in Fig. 9, which clearly reveals the non-Newtonian features [36]. In addition, shear-thinning behavior was exhibited by the co-gel samples. The data presented in Fig. 9 could be adequately

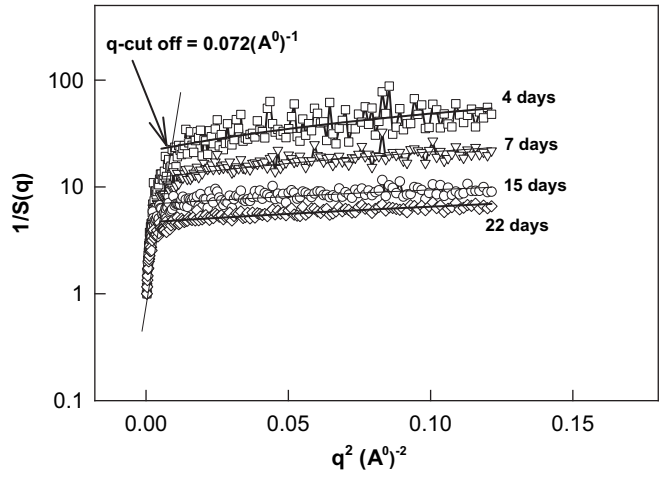

Fig. 6. SANS data on agar-gelatin co-gels taken at room temperature showing network evolution with gel age. Below q-cutoff data were least square fitted to Debye–Bueche and above q-cutoff to Ornstein–Zernike functions. See text for details.

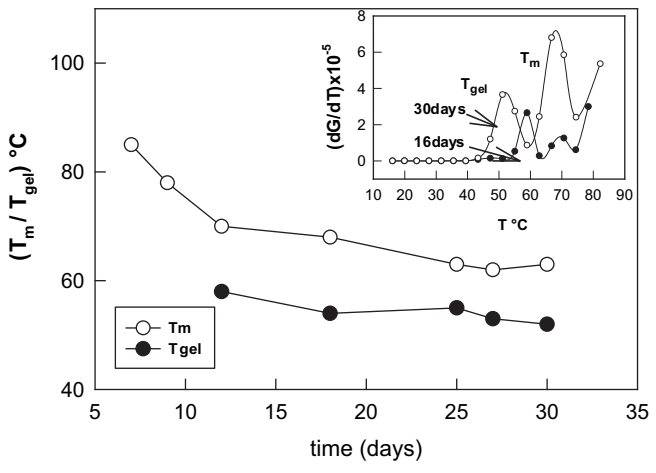

Fig. 7. Variation of agar-gelatin co-gel gelation and melting temperature with gel age determined from isochronal temperature sweep studies of storage modulus of the gel. The inset shows the first derivative of storage modulii with temperature. Solid lines are guide to eye.

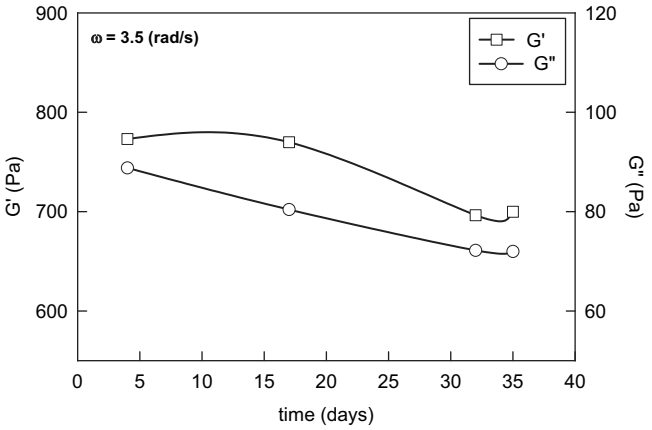

Fig. 8. Variation of isochronal storage and loss modulii of agar-gelatin co-gel sample with gel age determined from frequency sweep studies, performed at room temperature. The reduction in G′ and G″ was 10% and 20% respectively. Solid lines are guide to eye.

described through the power-law model [36] using the scaling relation

$$\eta(\gamma^{\bullet}) \sim (\gamma^{\bullet})^{-k} \tag{9}$$

The least-squares fitting yielded $k = 1.01 \pm 0.02$ for $1\ s^{-1} < \gamma^{\bullet} < 100\ s^{-1}$. In fact, k accounts for the viscous response of the samples to applied shear: $k = 0$ gives Newtonian, $k < 0$ indicates shear thickening and $k > 0$ implies shear-thinning behavior. Thus, shear-thinning features are clearly manifested in these samples independent of gel age. The drop in viscosity value observed at higher shear rates could correspond to the shear induced rupture of the weak network structures present in the system. Preferential alignment of these networks along the direction of applied shear can have similar effect.

In a network of connected chains, the shear modulus is proportional to the concentration of inter-molecular bonds. The value of the length of elastically active strands is similar to the characteristic viscoelastic network size, ζ_{el}, estimated from the low frequency shear modulus, G_0. This is true only when shear storage modulus of co-gel sample is weakly dependent on frequency, a fact established in our studies (data not shown). Thus, G_0 is a measure of elastic free-energy stored per unit volume of a characteristic viscoelastic network of size, ζ_{el}. This implies [37,38]

$$G_0 \sim k_B T/\zeta_{el}^3 \tag{10}$$

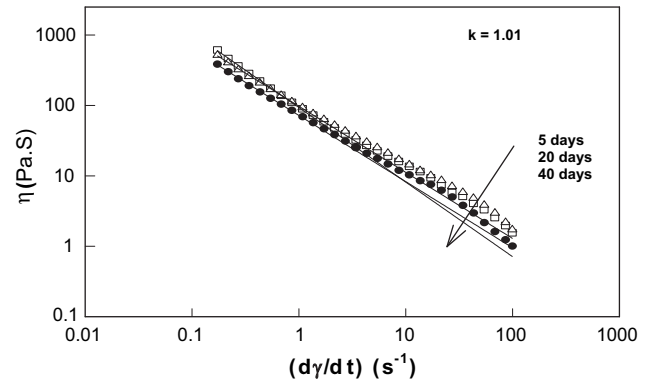

Fig. 9. Variation of shear viscosity with applied shear rate for agar-gelatin co-gel sample, and its dependence on gel age determined from flow mode rheological studies, performed at room temperature. The data could be fitted to the power-law: $\eta(\gamma^{\bullet}) \sim (\gamma^{\bullet})^{-k}$ with $k = 1.01 \pm 0.07$.

Thus, typical viscoelastic length scale prevalent in these materials becomes easily accessible from oscillatory rheology measurements. The viscoelastic length calculated from the measured value of G_0 is plotted in Fig. 3 as function of gel age which interestingly shows invariance.

3.5 Time-dependent re-organization and phase separation

Gelation, in a system containing a single or multiple types of polymers dispersed in a continuous phase (solvent), occurs following nucleation and growth dynamics or spinodal decomposition pathways [39]. Sol-gel transition is a phase transition from an ergodic to a non-ergodic state of the system. The nucleation and growth process differs from spinodal by the different development of concentration fluctuations. Near the bimodal tie-point, where nucleation and growth occurs, small concentration fluctuations are sustained as long as they are smaller than a critical size. On the other hand a nucleus having a size larger than the critical size is stable, but begins to coarsen immediately. Concentration fluctuations of certain wavelength specifically lower the free-energy of the system, and therefore, are preferred. This gives rise to the existence of characteristic length scales in the structure. Thus, the pattern of coarsening (length scale growth) bears the signature of the phase separation mechanism active in a system. Typically, the length scale, $L(t)$ scales with time as

$$L(t) \sim t^{\alpha} \tag{11}$$

For diffusive [40,41] and droplet coalescence processes [42], $\alpha = 1/3$ whereas in the asymptotic region characterized by broad interfacial width [43–46], this exponent becomes ¼. In processes where the convective flow gets coupled with droplet motion (hydrodynamic coarsening mechanism) this exponent can assume a value [47] $\alpha = 1$. Phase separation driven by spinodal decomposition is often characterized by $\alpha = 1/3$ and 1. Processes obeying nucleation and growth kinetics can yield [48] $\alpha = 1/10$. In crosslinked networks and gels the application of the kinetics of phase separation through coarsening described above becomes questionable. Because of the presence of crosslinks diffusion becomes severely constrained, the solvent bound to the network and trapped inside it as interstitial liquid effects droplet coalescence significantly. It has been shown that network elasticity cancels surface tension effects in gels [49] yielding a much lower coarsening exponent

$$\alpha = 1/3 - A\nu \tag{12}$$

where A is a constant and ν is crosslink density. In case of physical gels like gelatin and agar a clear definition of ν can be elusive.

Let us discuss agar-gelatin co-gel system under the aforesaid framework. Gelatin forms thermoreversible hydrogels (gelation temperature ≈30 °C) comprising inter twined triple helices stabilized by inter-helix hydrogen bonds. These gels do not exhibit syneresis, their heating and cooling curves overlap (no hysteresis), and the gelation process is adequately described by nucleation and growth model [25]. On the other hand, agar hydrogels exhibit syneresis and hysteresis (cooling and heating curves do not overlap). The gel comprises of right handed double helices stabilized by intermolecular hydrogen bonds and these supramolecular structures aggregate to form polymer-rich domains [26]. Agar gels are characterized by a distinct gelation temperature ≈37 °C and melting temperature ≈80 °C. The dynamics of sol-gel transition in agar has been described through spinodal decomposition [25]. Thus, the agar-gelatin co-gel system constitutes a complex system where the two processes, nucleation and growth, and spinodal decomposition, are in competition. We observed that syneresis was

active in this system. The quantitative study of the experimental data implies the following time-dependent behaviour. Two characteristic length scales could be extracted from the static (SANS) and dynamic (DLS) structure factor data given by the parameters: ξ_{SANS} and ξ_{DLS} as inhomogeneity size and ξ_C as correlation length.

The inhomogeneity size values obtained from SANS and DLS data (see Fig. 3) were found to scale with time (aging), t_a as

$$\xi_{SANS,DLS} = \xi_0 t_a^{-\alpha} \tag{13}$$

with $\xi_0 = 28 \pm 3$ nm and $\alpha = 1/5 \pm 0.04$. The coarsening exponent would imply, $A\nu \approx 0.1$ which gives an indication of the extent of cross-linking present in the system. The observed low coarsening exponent (1/5 as compared to 1/3 predicted for spinodal decomposition) can arise due to the presence of multiple coarsening regimes in a non-equilibrium gel that is slowly moving towards equilibrium following spinodal decomposition [50]. The correlation length determined from SANS data showed a decrease of 40% over the same period of aging. The slow mode relaxation frequency $(1/\tau_s)$, and the width of the slow mode structure factor (β) exhibited the following universal time dependence (Fig. 4)

$$(1/\tau_s) \text{ and } \beta \sim t_a^{-3/5} \tag{14}$$

Universal aging features observed in restructuring fractal gels revealed an universal power-law behaviour [3], $\tau_s \sim t_a^{0.9}$ as compared to $t_a^{0.6}$ observed in this work It can be argued that presence of syneresis plays a significant role in controlling time-dependent the structural evolution of colloidal gels. The difference in the two exponent values can be attributed to this.

Normally, syneresis induces gel to deform continuously and uniformly with time (aging). However, it has been suggested that gel adhesion to cell walls can cause localized stress and deformations tend to become non-uniform [3], and the system remains trapped in a non-ergodic state for a very long period of time. The existence of such a scenario was clearly seen in our case. The extent of non-ergodicity present in the co-gel was adequately described by the X-parameter plotted in Fig. 1 as function of time. It is seen that over a period of ≈30 days, the X-value remained invariant of gel aging indicating the slowness of the non-equilibrium to equilibrium transition. However, the macroscopic structural feature, given by the shear rate dependent viscosity data (Fig. 9) indicated the non-Newtonian viscoelastic behaviour that was found to be independent of gel aging. The gel melting temperature (≈85 °C) was indicative of agar when the nascent gel was formed which reduced to ≈55 °C after ≈25 days implying the formation of agar-gelatin complex networks. However, the gelation temperature of co-gel was consistently observed to be higher than agar gels. We did not observe any endotherm close to gelation temperature of gelatin implying that most probably gelatin gels were never formed in the co-gel. Such an observation is in consistence with earlier reports on agar-κ-carrageenan [13] and agar-gelatin [14] mixed gels. In the agar-κ-carrageenan [13] co-gel distinct agar and κ-carrageenan regions were formed yielding a discontinuous co-gel due to phase separation. In agar-gelatin co-gel system clearly partitioned domains of agar and gelatin-rich phases were observed in light and electron microscopy data which also revealed guest-host phase inversion features [14]. Thus, there seems to be a general tendency for agar molecules to phase separate into agar-rich domains where there is a propensity of double helix structures. Our experimental results, when combined with such observations, indicate that this phase segregation dynamics is governed by a spinodal decomposition mechanism. Finally, it was felt imperative to compare the physical characteristics of agar-gelatin co-gel with that of agar and gelatin gels, and their coacervate. Such a data is presented in Table 1. A cursory observation reveals that: (i) the characteristic length scales in agar-gelatin gels and coacervates are not too different, (ii) the thermal and mechanical features are fully dictated by agar only, and (iii) the viscoelastic features are identical for normal gels, their co-gels and corresponding coacervates which is remarkable. It is not clear at this stage why the correlation length values obtained for coacervate and co-gel samples were so small.

The coherent picture that emerges is the following. In the nascent state, as the hot mixed sol is cooled to room temperature, there is a competition between the agar and gelatin molecules to form agar gels with intermolecular hydrogen bonding, and agar-gelatin intermolecular complexes through electrostatic interactions (agar is polyanionic and gelatin has net positive charge). Since the physical gelation is a free-energy driven process, the gelation of agar continues until all accessible pair of molecules are joined together to form right handed double helices, aggregation of these in to network structure, and their concomitant re-organization via spinodal decomposition [25,26]. This creates agar-rich domains seen in the micrographs of ref.[14]. The gelatin molecules are phase separated into compartments that still contain unreacted agar molecules, and some of these localized zones might contain gelatin above its gelation concentration. However, probability of formation of gelatin triple helices is much smaller than that of formation of agar-gelatin complexes because, formation of a triple-helix involves three-body interactions whereas the same for a complex involves two-body contact. The electrostatic binding sites provide the junction zones for the growing networks. Typically, gelatin and agar gels have storage moduli values ≈340 Pa and 910 Pa whereas their co-gel modulus was ≈770 Pa which indicated that co-gel was softer than agar. Thus, there is a propensity of agar double helices in agar-rich domains comprising continuous phase, and the ungelled gelatin and agar molecules preferentially form complex networks in gelatin-rich regions that are non-uniformly distributed in space. Such a gel is heterogeneous and is trapped in a non-ergodic state, and in order to minimize the free-energy it must reorganize its internal structure with time and asymptotically approach equilibrium. The existence of syneresis facilitates this. The net effect of such a heterogeneous assembly is the softening of the co-gel with aging as characterized by the reduced melting temperature and gel modulii data. The said mechanism has been qualitatively observed

Table 1
Summary of physical characteristics describing various condensed phases of agar and gelatin. Data reported pertain to 25 °C for samples prepared in aqueous medium (D_2O for SANS experiments). The values listed are representative. The transition temperatures are associated with an uncertainty of ±3 °C and the same with characteristic sizes is ±15% of the listed data, typically. The physical property data for gelatin and agar gels have been collected from various previously reported works that are cited in ref.[6].

Sl No.	Parameter/ property	Gelatin gel[6]	Agar gel[6]	Agar-gelatin[6] Coacervate	Agar-gelatin co-gel (initial)
1.	Mesh size	2.6 nm	5.9 nm	1.2 nm	1.7 nm
2.	Size of heterogeneity	20 nm	70 nm	22 nm	21 nm
3.	First Transition Temp. (DSC)	28 °C	41 °C	30 °C	–
4.	Second Transition Temp. (DSC)	–	75 °C	75 °C	–
5.	First Transition Temp. (Rheology)	28 °C	35 °C	33 °C	–
6.	Second Transition Temp. (Rheology)	–	80 °C	80 °C	85 °C
7.	Viscoelastic Feature $\eta(\gamma^{\bullet}) \sim (\gamma^{\bullet})^{-k}$	Viscoelastic $k = 1.1$	Viscoelastic $k = 1.0$	viscous $k = 1.2$	Viscoelastic $k = 1.01$

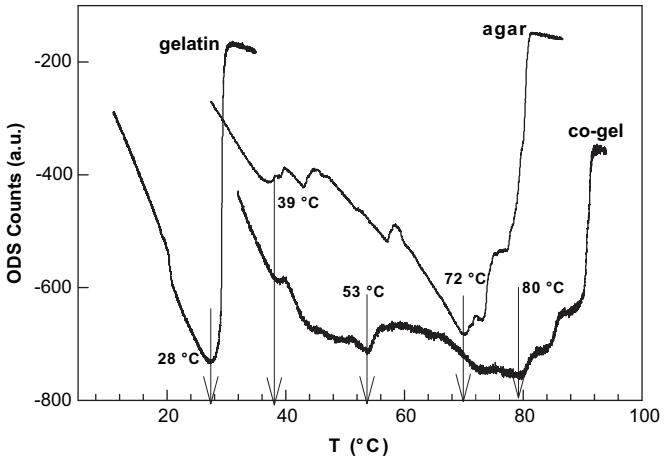

Fig. 10. Optical DSC data for agar and gelatin gels, and their co-gel samples obtained by heating the samples at the rate of 2 °C/min. The polymer concentrations were fixed at 1.5% w/v.

in a variety of physical co-gels like: agar-κ-carrageenan [13], agar-gelatin [14], gelatin-maltrodextrin [46], pectin-chitosan [4], β-glucan-sodium caseinate [12] etc. Interestingly, the slow dynamics and spinodal decomposition kinetics developed for glassy systems, and model colloidal gels [1–3] adequately describe the characteristic phase separation features observed in physical co-gels.

In order to probe the possible existence of complex network structures in co-gel samples, we performed DSC studies on these samples using an optical DSC instrument and the custom made Lynksys-32 control and analysis software (Linkam Scientific Instruments, England). An arbitrary mass of gel sample was loaded in an aluminum pan that was sealed with crimping. The co-gel sample used was 30 days old. The thermograms are shown in Fig. 10. Gelatin showed a characteristic gelation temperature, $T_{gel} \approx 28$ °C; agar sample yielded a gelation temperature, $T_{gel} \approx 40$ °C and a melting temperature, $T_m \approx 72$ °C. Interestingly, the co-gel sample exhibited endotherms corresponding to gelation, $T_{gel} \approx 40$ °C, $T_m \approx 72$–80 °C (Fig. 7 data for these values are 46 °C and 72 °C respectively), and in this temperature window the thermogram looked completely different from that of agar gel data. The weak endotherm seen at ≈53 °C for agar gel manifested itself as a broad endotherm in co-gel data. Similarly, the co-gel melting endotherm was much broader and it needs to be noted that the thermal signature of gelatin was completely missing in the co-gel thermogram. The coherent picture that emerges is that the gelatin molecules formed complex network with agar molecules thus loosing their identity, and presence of these structures is responsible for the differential features seen in co-gel data as compared to that of agar gel.

4. Conclusions

Two biopolymers, one a polysaccharide another a polypeptide were mixed in the sol state to allow simultaneous formation of a gel network of agar and complex network of agar-gelatin. The temporal evolution of the phase stability of this system was monitored. The results heavily rely on DLS and SANS data. The various scattering moieties describe characteristic sizes that evolved with time. These length scales have been speculatively associated with different physical dimensions of the polymers concerned. The "speeding up" of the fast and "slowing down" of slow mode indicated characteristic relaxations associated with this co-gel. The coarsening exponent of the characteristic length scale, ξ_{SANS} and ξ_{DLS}, implied the existence of multiple coarsening domains confined in a non-equilibrium and non-ergodic ensemble that slowly relaxed to equilibrium in a bid to minimize the free-energy and attain equilibrium. Evidence of spinodal decomposition mediated phase separation in polymer solutions with severely restricted diffusion rates, has been noted in earlier reports [51]. The slow dynamics associated with the temporal evolution of gels has been compared with the same of glassy systems [1]. It appears that at the microscopic level, syneresis arising from the free-energy driven self-organization of agar double helix structures tend to form aggregated domains through specific interactions. This enables the formation of agar-rich gel phase and the ungelled complex network of agar and gelatin molecules. These ungelled domains undergo osmotic swelling due to the availability of solvent in the local environment, there by, making the co-gel sufficiently soft and heterogeneous. This imparts a bi-continuous topology that is thermally stable, but structurally not. Thus, the structure of the inhomogeneous gel continues to evolve with time by self-generated internal stress [1–3]. Interestingly, similar features have been observed in another class of soft matter, called coacervates [51]. It must be realized that there has not been enough experimental investigations to probe these phenomenon in depth, and to establish their universality. The results presented provide a significant insight into the distinctive micro-structural features of agar-gelatin co-gel that dynamically evolves with time this paper does not answer all the questions related to the structure of such complex systems, yet it makes an attempt to give some foundation to its understanding. The issue of dependence of various characteristic size parameters on polymer concentration and mixing ratio remains unresolved at this stage.

Acknowledgement

S. Santinath Singh is thankful to University Grants Commission, India, for a senior research fellowship. This work was supported by a Department of Science Technology, Government of India, and research grant. The neutron beam time was made available through a collaborative research scheme (UGC-DAE-CSR) of Department of Atomic Energy, Government of India.

References

[1] (a) Tanaka H, Jabbari-Farouji S, Meunier J, Bonn D. Phys Rev E 2005;71:021402–12;
(b) Tanaka H, Jabbari-Farouji S, Meunier J, Bonn D. Phys Rev E 2004;69:031404–10.
[2] Fluerasu A, Moussaid A, Madsen A, Schofield A. Phys Rev E 2007;76:010401R–5.
[3] Cipelletti L, Manley S, Ball RC, Weitz DA. Phys Rev Lett 2000;84:2275–8.
[4] Nordby MH, Anna-Lena Kjoniksen, Nystrom B, Roots J. Biomacromolecules 2003;4:337–43.
[5] Ferri F, Greco M, Arcovito G, Andresai Bassi F, De Spirito M, Paganini E, et al. Phys Rev E 2001;63:031401–17.
[6] Singh SS, Aswal VK, Bohidar HB. Int J Biol Macromol 2007;41:301–7.
[7] Kayitmazer AB, Bohidar HB, Mattison KM, Bose A, Sarkar J, Hashidzume A, et al. Soft Matter 2007;3:1064–76.
[8] Mohanty B, Amarnath Gupta, Bandyopadhyay S, Bohidar HB. J Polym Sci Part-B (Physics) 2007;45:1511–20.
[9] Mohanty B, Aswal VK, Kohlbrecher J, Bohidar HB. J Polym Sci Part-B (Physics) 2006;44:1653–67.
[10] Kayitmazer AB, Strand SP, Tribet C, Bose A, Jaeger W, Dubin PL. Biomacromolecules 2007;8:3568–77.
[11] Bohidar HB, Dubin PL, Osada Y. Polymer gels: fundamentals and applications. Washington, DC: American Chemical Society; 2002. Vol. 833.
[12] Kontogiorgos V, Ritzoulis C, Biliaderis CG, Kasapis S. Food Hydrocolloids 2006;20:749–56.
[13] Norziah MH, Foo SL, Karim AA. Food Hydrocolloids 2006;20:204–6.
[14] Clark AH, Richardson RK, Ross-Murphy RK, Stubbs JM. Macromolecules 1983;16:1367–74.
[15] Watase M, Nishinari K. Rheol Acta 1980;19:220–5.

[16] Soloukhin VA, Brokken-Zijp JCM, van Asselen OJ, de With G. Macromolecules 2003;36:7585–97.
[17] Hunt AJ, Ayers MR. J Non-Cryst Solids 2001;85:162–6.
[18] Rao VA, Rao PA, Kulkarni MA. J Non-Cryst Solids 2004;350:224–9.
[19] Kotani Y, Matsuda A, Tatsumisago M, Minami TJ. J Mat Chem 2000;10:2765–8.
[20] Mellema M, Heesakkers WM, van Opheusden JHJ, van Bilet T. Langmuir 2000;16:6847–54.
[21] Flora KK, Brennan JD. Chem Mater 2001;13:4170–9.
[22] Alata H, Aoyama T, Inoue Y. Macromolecules 2007;40:4546–51.
[23] Veis A. The macromolecular chemistry of gelatin. New York: Academic Press; 1964.
[24] Craigie JS, Leigh C. In: Hellebust JA, Craigie JS, editors. Hand book of phycological methods. Cambridge: Cambridge; 1978. p. 109.
[25] Pines E, Prins W. Macromolecules 1972;6:888–95.
[26] Jung-Ying Xiong, Narayanan J, Xiang-Yang Liu, Chong TK, Chen Chung SB. J Phys Chem B 2005;109:5638–43.
[27] Thiyagaranjan P, Epperson JE, Crawford RK, Carpenter JM, Klippert TE, Wozniak DG. J Appl Crstyllogr 1997;30:280–93.
[28] (a) Geissler E. In: Brown W, editor. Dynamic light scattering. London: Oxford; 1993; (b) Coviello T, Geissler E, Meier D. Macromolecules 1997;30:2008–15.
[29] Sharma J, Bohidar HB. Colloid Polym Sci 2000;278:15–21.
[30] Pusey PN. Macromol Symposia 1994;79:17;
Pusey PN, Van Megen W. Physica A 1989;157:705–41.
[31] Bohidar HB. Characterization of polyelectrolytes by dynamic light scattering, handbook of polyelectrolytes-II. California: American Scientific Publishers; 2002.
[32] Ren SZ, Sorensen CM. Phys Rev Lett 1993;70:1727–30.
[33] Singh SS, Siddhanta AK, Meena Prasad K, Bandyopadhyay S, Bohidar HB. Int J Biol Macromol 2007;41:185–92.
[34] Uematsu T. Phys Rev E 2003;68:051803–11.
[35] (a) de Gennes PG. Scaling concepts in polymer physics. Ithaca, USA: Cornell University Press; 1985;
(b) Debye P, Bueche AMJ. Appl Phys 1949;20:518–35.
[36] Barnes HA. A handbook of elementary rheology. Wales, England: University of Wales Press; 2000.
[37] Ajji A, Choplin L. Macromolecules 1991;24:5221–3.
[38] Strobl G. Physics of polymers. Berlin, Germany: Springer; 1997.
[39] Tokuyama M, Kawasaki K. Physica A 1984;123:386–411.
[40] Bray AJ. Phys Rev Lett 1989;62:2841–4.
[41] Tanaka H. J Phys:Condens Matter 2000;12:R207–64.
[42] Mazenko GF. Phys Rev Lett 1989;63:1605–8.
[43] Mouritsen OG. Phys Rev B 1985;37:2613–6.
[44] Rogers TM, Desai RC. Phys Rev B 1989;39:11956–64.
[45] Rogers TM, Elder KR, Desai RC. Phys Rev B 1988;37:9638–49.
[46] Siggia ED. Phys Rev A 1979;20:595–605.
[47] Tanaka H, Yokokawa T, Abe H, Hayasi T, Nishi T. Phys Rev Lett 1990;65:3136–9.
[48] Onuki A, Puri S. Phys Rev E 1999;59:R1331–4.
[49] Butler MF. Biomacromolecules 2002;3:676–83.
[50] van Aartsen JJ, Smolders C. Eur Polym J 1970;6:1106–12.
[51] Mohanty B, Bohidar HB. Europhys Lett 2006;76:965–71.